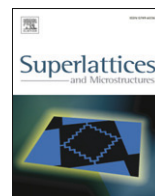




ELSEVIER

Contents lists available at ScienceDirect

Superlattices and Microstructures

journal homepage: www.elsevier.com/locate/superlattices

Third-harmonic generation in asymmetric coupled quantum wells

Rui-Zhen Wang, Kang-Xian Guo*, Bin Chen, Yun-Bao Zheng, Bin Li

Department of Physics, College of Physics and Electronic Engineering, Guangzhou University, Guangzhou 510006, PR China

ARTICLE INFO

Article history:

Received 3 April 2008

Received in revised form

11 September 2008

Accepted 6 October 2008

Available online 22 November 2008

Keywords:

Third-harmonic generation

Asymmetric coupled quantum wells

Quantum confinement effect

ABSTRACT

The third-harmonic generation (THG) in asymmetric coupled quantum wells (ACQWs) for different values of the well parameter Δ and width of barrier (W_B) are theoretically studied. The analytical expression of the third-harmonic generation is derived by using the compact density-matrix approach and the iterative method. Finally, the numerical calculations are presented for typical GaAs/Al_xGa_{1-x}As asymmetric coupled quantum wells. Results obtained show that the third-harmonic generation in the asymmetric coupled quantum wells can be importantly modified by the parameter Δ and W_B . Moreover, third-harmonic generation also depends on the relaxation rate of the asymmetric coupled quantum wells.

© 2008 Elsevier Ltd. All rights reserved.

1. Introduction

As we know, nonlinear effects can be enhanced dramatically in the low-dimension of quantum systems than that in bulk materials due to the existence of a quantum confinement effect. So much attention has been paid to the nonlinear optical properties of low-dimensional semiconductor structures in both theoretical and the applied physics in the past few years [1–18]. Low-dimensional semiconductor structures include quantum wells, superlattices and nanostructures and so on. Among the nonlinear optical properties, more and more attention had been paid to second-order nonlinear properties [5,19,20], such as optical rectification (OR) [4,13,16,21], second-harmonic generation (SHG) [12,19,22], electro-optic effect (EOE) [10], third-harmonic generation (THG) [23–25]. As we know second- and third-harmonic generations are very important since those nonlinearities have potential for device applications in far infrared laser amplifiers, photo-detectors, and high-speed electro-optical modulators.

* Corresponding author. Tel.: +86 13342886687.

E-mail address: axguo@sohu.com (K.-X. Guo).

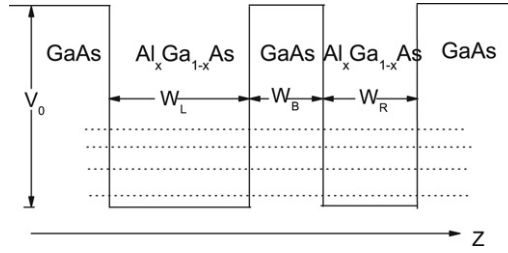


Fig. 1. Schematic diagram for electronic confined potential profile and the two bound energy-levels in an asymmetric coupled GaAs/ $\text{Al}_x\text{Ga}_{1-x}\text{As}$ quantum wells.

In most previous works, an asymmetric quantum well structure was used to obtain a large third-order nonlinear effect and asymmetric quantum well structures such as compositionally asymmetric quantum wells [22,26], asymmetrically coupled quantum wells [27,28] and applied-field biased quantum wells [29] were used widely in experiments. Many authors calculated the SHG, OR, EOE, THG coefficient in single quantum wells. In 2003, bound states and third-harmonic generation in a semi-parabolic quantum well with an applied electric field was studied by Li Zhang and Hong-Jing Xie [30]. The strength of the THG susceptibility in the asymmetric quantum well can reach a magnitude of 10^{-13} (m/V)². In Ref. [31], Capasso et al. have reported that they experimentally achieved a magnitude of 10^{-14} (m/V)² in a coupling quantum well. However, the THG has not been studied in asymmetric coupled quantum wells (ACQWs) system. So it is worth paying much attention to the THG in asymmetric coupled quantum wells. The purpose of this paper is to study the influence of the parameters of Δ and width of barrier effect on the THG. Δ represents the width difference between the left well and the right well.

In this paper, the THG susceptibility in the GaAs/ $\text{Al}_x\text{Ga}_{1-x}\text{As}$ ACQWs is investigated. In Section 2, with the compact density matrix approach and iterative method, the Hamiltonian, relevant eigenstates and eigenenergies, and the analytical expression of the THG susceptibility are described. In Section 3, numerical results are presented for GaAs/ $\text{Al}_x\text{Ga}_{1-x}\text{As}$ ACQWs. Finally, brief conclusions are given in Section 4.

2. Theory

Fig. 1 shows the schematic diagram for electronic confined potential profile in ACQWs. The effective-mass Hamiltonian for the electron in ACQWs system is

$$H = -\frac{\hbar^2}{2m^*} \left[\frac{\partial^2}{\partial x^2} + \frac{\partial^2}{\partial y^2} + \frac{\partial^2}{\partial z^2} \right] + V(z) \quad (1)$$

with

$$V(z) = \begin{cases} V_0, & z < -(W_L + W_B/2), -W_B/2 \leq z \leq W_B/2, z > W_B/2 + W_R \\ 0, & \text{elsewhere} \end{cases} \quad (2)$$

for ACQWs. Where z represents the growth direction of this quantum wells, \hbar is Planck's constant, m^* is the conduction-band effective mass, and V_0 is the profile of the conduction-band potential in the quantum wells. W_L , W_R and W_B represent the width of the left well, the width of the right well and the width of the barrier, respectively. By solving the Schrödinger equation $H\psi_{n,k}(r) = e_{n,k}\psi_{n,k}(r)$, the eigenfunctions $\psi_{n,k}(r)$ and the eigenenergies $e_{n,k}$ are given by

$$\psi_{n,k}(r) = \varphi_n(z)u_c(r)e^{ik_{\parallel} \cdot r_{\parallel}}, \quad (3)$$

and

$$e_{n,k} = E_n + \frac{\hbar^2}{2m^*} |k_{\parallel}|^2. \quad (4)$$

Here, k_{\parallel} and r_{\parallel} are the wave vector and coordinate in the x - y plane and $u_c(r)$ is the periodic part of the Bloch function in the conduction band at $k = 0$. $\varphi_n(z)$ and E_n are the solution of the one-dimensional Schrödinger equation

$$H_z \varphi_n(z) = E_n \varphi_n(z). \quad (5)$$

where H_z is the z component of the whole Hamiltonian H , and it is given by

$$H_z = -\frac{\hbar^2}{2m^*} \frac{d^2}{dz^2} + V(z). \quad (6)$$

Solving this equation, the bound states can be given as follows,

$$\varphi_n(z) = \begin{cases} A \exp\{kz\} \\ B_1 \cos\{k'z\} + B_2 \sin\{k'z\} \\ C_1 \exp\{-kz\} + C_2 \exp\{kz\} \\ D_1 \cos\{k'z\} + D_2 \sin\{k'z\} \\ G \exp\{-kz\} \end{cases} \quad (7)$$

with the wave vectors given by $k = \sqrt{2m^*(V-E)}/\hbar$ and $k' = \sqrt{2m^*E}/\hbar$, where E_n is the corresponding energy level, $A, B_1, B_2, C_1, C_2, D_1, D_2$ and G are the normalized coefficients of the wave function. All those normalized coefficients and the eigenenergy E_n can be numerically solved by the standard boundary condition of the electronic bound state.

Now, we will present a formalism for the nonlinear THG in ACQWs. Let us consider an electromagnetic field with frequency ω which is incident with a polarization vector normal to the quantum wells. The system is excited by an electromagnetic field $E(t) = \tilde{E}e^{-i\omega t} + \tilde{E}^*e^{i\omega t}$. Let us denote ρ as the one-electron density matrix for this regime. Then the evolution of the density matrix ρ obeys the following:

$$\frac{\partial \rho_{ij}}{\partial t} = \frac{1}{i\hbar} [H_0 - qzE(z), \rho]_{ij} - \Gamma_{ij}(\rho - \rho^{(0)})_{ij}. \quad (8)$$

where H_0 is the Hamiltonian for this system without the incident field $E(t)$, q is the electronic charge, $\rho^{(0)}$ is the unperturbed density matrix and Γ_{ij} is the relaxation rate. Eq. (8) is solved by using the usual iterative method [3,19]:

$$\rho(t) = \sum_n \rho^{(n)}(t). \quad (9)$$

with

$$\frac{\partial \rho_{ij}^{(n+1)}}{\partial t} = \frac{1}{i\hbar} \left\{ [H_0, \rho^{(n+1)}]_{ij} - i\hbar \Gamma_{ij} \rho_{ij}^{(n+1)} \right\} - \frac{1}{i\hbar} [qz, \rho^{(n)}]_{ij} E(t). \quad (10)$$

The electronic polarization of the square quantum wells can be expanded as Eq. (9). We will restrict ourselves to considering the first third orders, i.e.

$$P(t) = \varepsilon_0 \left(\chi_{\omega}^{(1)} \tilde{E} e^{i\omega t} + \chi_{2\omega}^{(2)} \tilde{E}^2 e^{2i\omega t} \right) + c.c. + \varepsilon_0 \chi_{3\omega}^{(3)} \tilde{E}^3 e^{3i\omega t}. \quad (11)$$

where $\chi_{\omega}^{(1)}$, $\chi_{2\omega}^{(2)}$ and $\chi_{3\omega}^{(3)}$ denote the linear, second-harmonic generation, and third-harmonic generation, respectively. ε_0 is the vacuum permittivity. The electronic polarization of the n th order is given by

$$P^{(n)}(t) = \frac{1}{S} \text{Tr}(\rho^{(n)} qz). \quad (12)$$

where S is the area of interaction.

In this paper, we lay emphasis on the calculation of the THG. By using the same compact density matrix approach and the iterative procedure as Ref. [18], we have calculated of the expression of $\chi_{3\omega}^{(3)}$ for this model:

$$\chi_{3\omega}^{(3)} = \frac{NM_{01}M_{12}M_{23}M_{30}}{\epsilon_0 \hbar^3} \left[\frac{1}{(3\omega - \omega_{21} - i\Gamma_{21})(2\omega - \omega_{20} - i\Gamma_{20})(\omega - \omega_{23} - i\Gamma_{23})} + \frac{1}{(3\omega - \omega_{21} - i\Gamma_{21})(2\omega - \omega_{20} - i\Gamma_{20})(\omega - \omega_{30} - i\Gamma_{30})} + \frac{1}{(3\omega - \omega_{23} - i\Gamma_{23})(2\omega - \omega_{20} - i\Gamma_{20})(\omega - \omega_{10} - i\Gamma_{10})} + \frac{1}{(3\omega - \omega_{30} - i\Gamma_{30})(2\omega - \omega_{20} - i\Gamma_{20})(\omega - \omega_{21} - i\Gamma_{21})} + \frac{1}{(3\omega - \omega_{30} - i\Gamma_{30})(2\omega - \omega_{31} - i\Gamma_{31})(\omega - \omega_{21} - i\Gamma_{21})} + \frac{1}{(3\omega - \omega_{01} - i\Gamma_{01})(2\omega - \omega_{31} - i\Gamma_{31})(\omega - \omega_{32} - i\Gamma_{32})} + \frac{1}{(3\omega - \omega_{21} - i\Gamma_{21})(2\omega - \omega_{31} - i\Gamma_{31})(\omega - \omega_{30} - i\Gamma_{30})} + \frac{1}{(3\omega - \omega_{21} - i\Gamma_{21})(2\omega - \omega_{31} - i\Gamma_{31})(\omega - \omega_{01} - i\Gamma_{01})} \right], \quad (13)$$

where N is the density of electrons in the quantum wells. ϵ_0 is the vacuum permittivity. $\omega_{ij} = (E_i - E_j)/\hbar$. $M_{ij} = e|\langle\varphi_j|r|\varphi_i\rangle|$ ($i, j = 0, 1, 2, 3$) is the off-diagonal matrix element.

3. Results and discussions

In this section, the third-harmonic generations are calculated numerically for the typical GaAs/Al_xGa_{1-x}As ACQWs. The parameters chosen in this work are [18,21,29]: $m^* = 0.067m_0$ (m_0 is the free-electron mass), $V = 228$ meV (corresponding to Al concentration $x = 0.3$), $\rho_s = 5 \times 10^{24} \text{ m}^{-3}$, $\hbar\Gamma_{30} = \hbar\Gamma/3$ (meV), $\hbar\Gamma_{10} = \hbar\Gamma_{21} = \hbar\Gamma_{32} = \hbar\Gamma$ (meV), $\hbar\Gamma_{20} = \hbar\Gamma_{31} = \hbar\Gamma/2$ (meV), $\Delta = W_L - W_R$.

In Fig. 2, we plot the third-harmonic generation $|\chi_{3\omega}^{(3)}|$ as a function of the photon energy $\hbar\omega$ for five different values of Δ with $W_L + W_R = 16$ nm, $W_B = 4$ nm. From this figure, it can be seen that, firstly, the THG susceptibilities are not a monotonic function of Δ . The strength of the THG susceptibility in the ACQWs can reach a magnitude of 10^{-12} , which is 1–2 orders higher than that in a single quantum well. Secondly, there is not only one peak position at different photon energy. The lower peak is mainly due to two-photon resonance enhancement. The higher peak originates from three-photon resonance enhancement. Finally, with increasing Δ , the peak of $|\chi_{3\omega}^{(3)}|$ has a blue-shift. This behavior can be attributed to the fact that the separation between the neighboring energy levels becomes wider as Δ is increasing. So the peak of $|\chi_{3\omega}^{(3)}|$ appears in the high-energy direction.

To understand the above phenomena more clearly, we plot the Fig. 3. Fig. 3 shows the third-harmonic generation $|\chi_{3\omega}^{(3)}|$ versus the parameter Δ for five different values of the photon energy $\hbar\omega$, $\hbar\omega = 0.0532, 0.0552, 0.0602, 0.0646, 0.0751$ eV, while $W_B = 4$ nm. It can be seen that with an increase of Δ , the peak of the $|\chi_{3\omega}^{(3)}|$ increases initially, and at $\Delta = 14$ nm, it reaches the maximum $8.9 \times 10^{-11} (\text{m/V})^2$, at this point, the asymmetric degree of ACQWs reach a maximum. We analyze this figure, and we can obtain that the asymmetric degree of ACQWs become stronger with Δ increasing at the beginning, then becomes weaker, subsequently, it increases with Δ increasing, at $\Delta = 14$ nm, the asymmetric degree reaches a maximum, then the asymmetric degree decreases smoothly. All these phenomena agree well with above results discussed in Fig. 2.

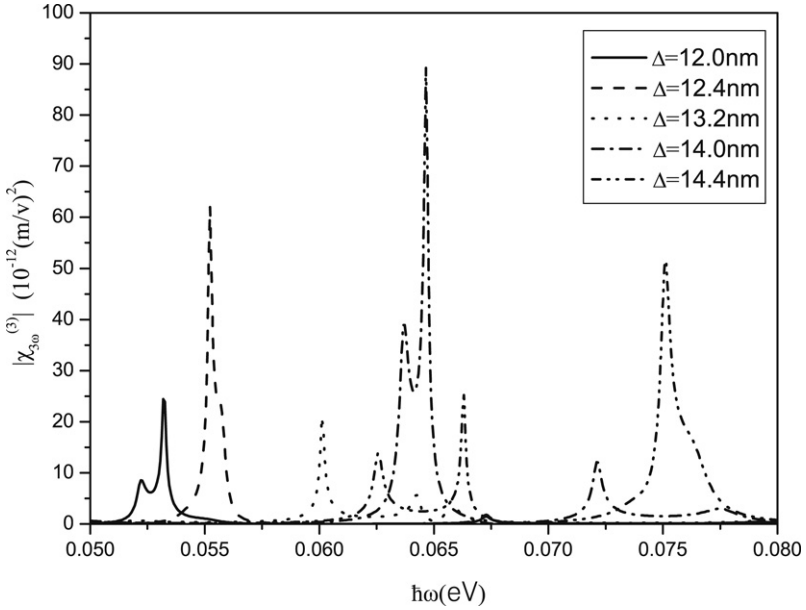


Fig. 2. The THG $|\chi_{3\omega}^{(3)}|$ as a function of the incident photon energy $\hbar\omega$ for five different values of Δ , $\Delta = W_L - W_R = 12, 12.4, 13.2, 14, 14.4$ nm, $W_L + W_R = 16$ nm, $W_B = 4$ nm.

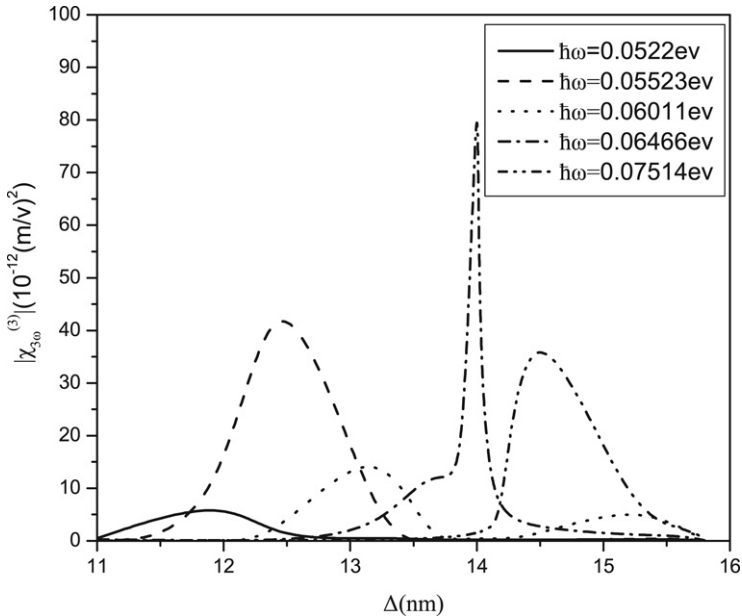


Fig. 3. The THG $|\chi_{3\omega}^{(3)}|$ as a function of the Δ for five different values of incident photon energy $\hbar\omega$, $\hbar\omega = 0.0532, 0.05523, 0.06011, 0.06466, 0.07514$, while $W_B = 4$ nm.

In Fig. 4, we plot the THG $|\chi_{3\omega}^{(3)}|$ as a function of the incident photon energy $\hbar\omega$ for five different values of the width of barrier W_B , $W_B = 3, 5, 6, 8, 10$, with $\Delta = 14$ nm. It can be seen that the THG susceptibilities are also not a monotonic function of W_B . The resonant peaks rise at first and become

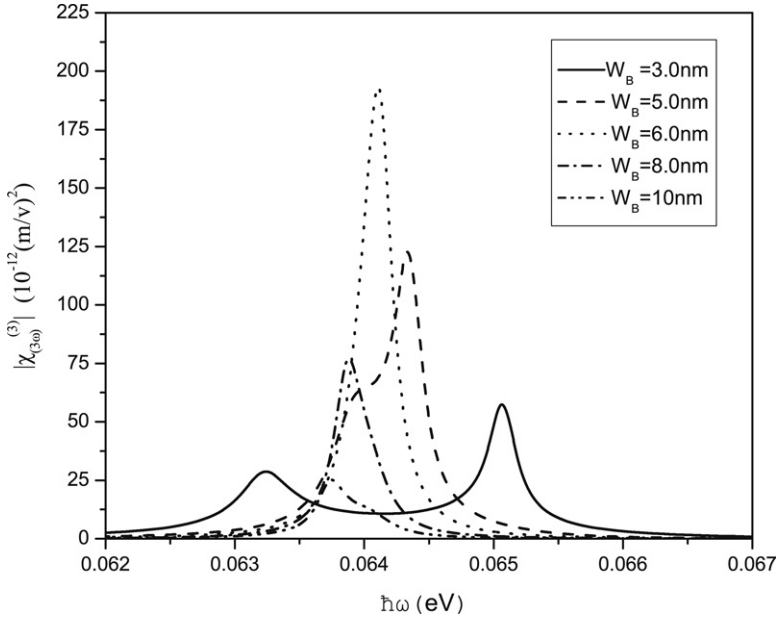


Fig. 4. The THG $|\chi_{3\omega}^{(3)}|$ as a function of photon energy $\hbar\omega$ for five different values of the width of barrier W_B , $W_B = 3, 5, 6, 8, 10$ nm, while $\Delta = 14$ nm.

sharpen, then falls as the incident photon energy $\hbar\omega$ is increasing. The peak can reach a magnitude of $10^{-10}(\text{m/V})^2$. Another important feature is that it can have two peaks while $W_B = 3$ nm. The higher peak near $\hbar\omega = 0.06321$ eV originates from the three-photon resonance enhancement, and the lower peak nearing $\hbar\omega = 0.06505$ eV is mainly due to two-photon resonance enhancement. We also observe the peak of the THG has a red shift with increasing W_B . This behavior can be attributed to the fact that the separation between the neighboring energy levels becomes narrower with W_B increasing. So the peak of $|\chi_{3\omega}^{(3)}|$ appears in the low-energy direction.

To illustrate the dependency relationship of $|\chi_{3\omega}^{(3)}|$ on W_B more clearly, we have plotted Fig. 5, which presents the THG $|\chi_{3\omega}^{(3)}|$ as a function of W_B for four different values of the incident photon energy $\hbar\omega$, $\hbar\omega = 0.06387, 0.06413, 0.06433, 0.06505$ eV, while $\Delta = 14$ nm. It can be seen from the figure that, with an increase of W_B , the $|\chi_{3\omega}^{(3)}|$ increases initially, it reaches the largest value, then it decreases. All these phenomena agree well with above results discussed in Fig. 4.

Fig. 6, we plot the THG $|\chi_{3\omega}^{(3)}|$ as a function of the photon energy $\hbar\omega$ for four different values of relaxation rates $\hbar\Gamma = 0.5, 0.7, 0.9, 1.1$ meV. The figure reveals that the relaxation rate has a great influence on the THG $|\chi_{3\omega}^{(3)}|$. It can be seen that the peak value will decrease as the relaxation rate increasing. We also observe that each curve has one peak at $\hbar\omega = 0.06407$ eV. It is due to three-photon resonance enhancement. The relaxation rate is not only related to the ACQWs material, but also to factors, such as temperature, boundary conditions, electron–electron and electron–phonon interactions.

4. Conclusion

We present a simple and straightforward method of the THG for an asymmetrical couple quantum well. Numerical calculations are performed for the typical GaAs/Al_xGa_{1-x}As coupled quantum wells, and the calculations mainly focus on the dependence of the THG $|\chi_{3\omega}^{(3)}|$ on the parameter Δ and the barrier, the incident photon energy and the relaxation rate of the ACQW system. Our results show that the theoretical value of $|\chi_{3\omega}^{(3)}|$ can reach a magnitude of $10^{-12}(\text{m/V})^2$ in this ACQW system.

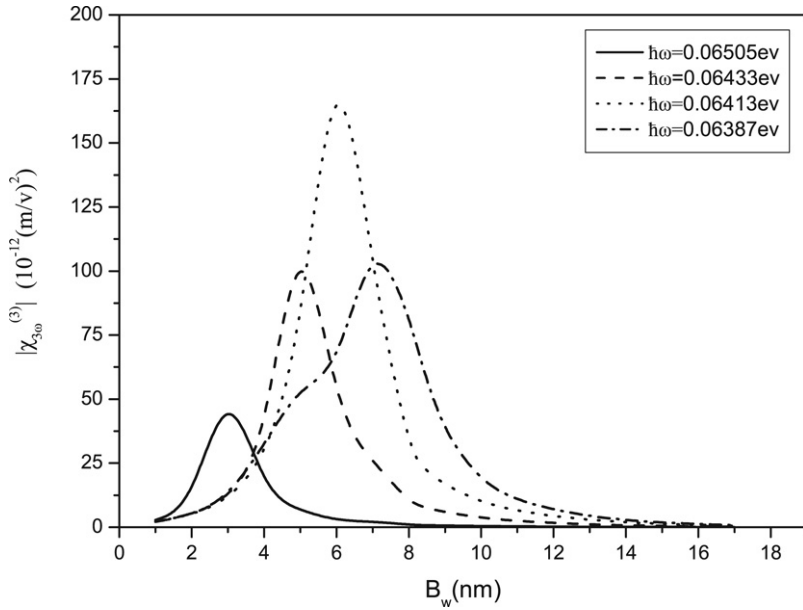


Fig. 5. The THG $|\chi_{3\omega}^{(3)}|$ as a function of the barrier W_B for four different values of the incident photon energy $\hbar\omega$, $\hbar\omega = 0.06387, 0.06413, 0.06433, 0.06505$ eV, while $\Delta = 14$ nm.

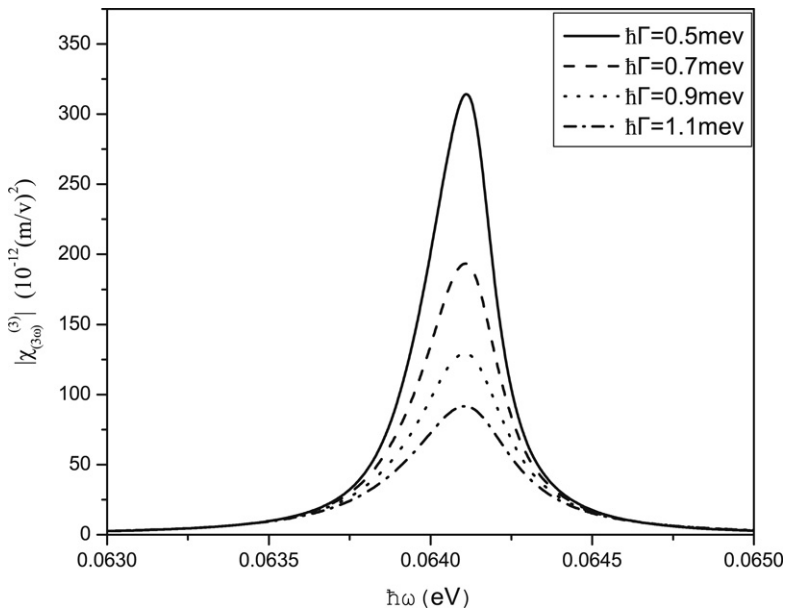


Fig. 6. The THG $|\chi_{3\omega}^{(3)}|$ as a function of the photon energy $\hbar\omega$ for four different relaxation rates $\hbar\Gamma = 0.5, 0.7, 0.9, 1.1$ meV, while $\Delta = 14$ nm, $W_B = 6$ nm.

We also find that THG is not a monotonic function of Δ and W_B . We can get a larger peak-value of $|\chi_{3\omega}^{(3)}|$ by choosing Δ and W_B appropriately, and a relatively low doped concentration. At last, we hope

theoretical investigations can make a great contribution to experimental studies, and may open new opportunities for optical exploitation of the quantum-size effect in devices.

Acknowledgments

This work is supported by the National Natural Science Foundation of China (under Grant no. 60878002), the Science and Technology Committee of Guangdong Province (under Grant nos. 2007B010600061, 2008B010200043, 2008B010600050 and 8251009101000002).

References

- [1] R. Atanasov, F. Bassani, V.M. Agranovich, *Phys. Rev. B* 50 (1994) 7809.
- [2] C. Sirtori, F. Capasso, D. Sivco, S. Chu, A. Cho, *Phys. Rev. B* 68 (1992) 1010.
- [3] E. Rosencher, Ph. Bois, *Phys. Rev. B* 44 (1991) 11315.
- [4] K.X. Guo, S.W. Gu, *Phys. Rev. B* 47 (1993) 16322.
- [5] J. Khurgin, *Phys. Rev. B* 38 (1988) 4056.
- [6] J. Khurgin, *Appl. Phys. Lett.* 51 (1987) 2100.
- [7] V. Milanovic, Z. Ikonc, *Solid State Commun.* 104 (1997) 445.
- [8] L. Tsang, Sh. Lee, *Phys. Rev. B* 41 (1990) 5942.
- [9] K.X. Guo, C.Y. Chen, *Acta Photon. Sin.* 28 (1999) 97.
- [10] Y.B. Yu, K.X. Guo, *Physica E* 18 (2003) 492.
- [11] T. Takagahara, *Phys. Rev. B* 36 (1987) 9293.
- [12] B. Li, K.X. Guo, C.J. Zhang, Y.B. Zheng, *Phys. Lett. A* 367 (2007) 493.
- [13] I. Karabulut, H. Safak, Mehmet Tomak, *Solid State Commun.* 135 (2005) 735.
- [14] K.X. Guo, C.Y. Chen, *Acta Photon. Sin.* 29 (2000) 501.
- [15] E. Hanamura, *Phys. Rev. B* 45 (1987) 1273.
- [16] I. Karabulut, H. Safak, *Physica B* 368 (2005) 82.
- [17] L. Zhang, Y.M. Chi, *Phys. Lett. A* 366 (2007) 256.
- [18] E. Ozturk, I. Sokmen, *Superlatt. Microstruct.* 41 (2007) 36.
- [19] C.J. Zhang, K.X. Guo, *Physica E* 33 (2006) 363.
- [20] K.X. Guo, C.Y. Chen, *Physica B* 269 (1999) 139.
- [21] E. Rosencher, P. Bois, J. Nagle, E. Costard, S. Dclaire, *Appl. Phys. Lett.* 55 (1989) 1597.
- [22] R. Atanasov, F. Bassani, *Phys. Rev. B* 7809 (1994) 56126.
- [23] Z.E. Lu, K.X. Guo, *Commun. Theoret. Phys.* 45 (2006) 171.
- [24] G.H. Wang, K.X. Guo, *Physica B* 315 (2002) 234.
- [25] C.J. Zhang, K.X. Guo, *Physica B* 383 (2006) 183.
- [26] S.J.B. Yoo, M.M. Fejer, R.L. Byer, J.S. Harris Jr., *Appl. Phys. Lett.* 58 (1991) 1724.
- [27] E. Rosencher, P. Bois, B. Vinter, J. Nagle, D. Kaplan, *Appl. Phys. Lett.* 56 (1990) 1822.
- [28] C. Sirtori, F. Cappasso, D.L. Sivco, S.N.G. Chu, A. Cho, *Appl. Phys. Lett.* 59 (1991) 2302.
- [29] M.M. Fejer, S.J.B. yoo, R.L. Byer, A. Harwit, J.S. Harrisjt, *Phys. Rev. Lett.* 62 (1989) 1041.
- [30] L. Zhang, H.J. Xie, *Phys. Rev. B* 68 (2003) 235315.
- [31] C. Sirtori, F. Capasso, D.L. Sivco, A.Y. Cho, *Phys. Rev. Lett.* 68 (1992) 1253.